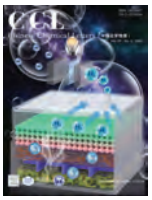
Chinese Chemical Letters 37 (2026) 111139

Contents lists available at ScienceDirect

Chinese Chemical Letters

journal homepage: www.elsevier.com/locate/cclet



Near-infrared light-activated switchable antibacterial agent based on dithienylethene photoswitch

Ziyong Li[a,1,*], Jinzhao Song[a,1], Qilian Wang[a], Yueheng Qi[a], Xingrui Gao[a], Yongliang Feng[a], Haining Zhang[a], Ying-Jun Chen[a], Hui Guo[a], Xiao-Gang Yang[a,*], Jun Yin[b,*]

[a] *Luoyang Key Laboratory of Organic Functional Molecules, College of Food and Drug, College of Chemistry and Chemical Engineering, Luoyang Normal University, Luoyang 471934, China*

[b] *National Key Laboratory of Green Pesticide, International Joint Research Center for Intelligent Biosensor Technology and Health, College of Chemistry, Central China Normal University, Wuhan 430079, China*

ARTICLE INFO

Article history:
Received 8 January 2025
Revised 20 March 2025
Accepted 24 March 2025
Available online 25 March 2025

Keywords:
Dithienylethene
Photochromism
Photopharmacology
Fluoroquinolones
Antibiotic resistance

ABSTRACT

The photopharmacology incorporated with molecular photoswitches offers a promising solution to fundamentally address the problem of bacterial resistance, simultaneously realizes the spatiotemporal precision treatment through remote light control. However, most of reported photoswitchable drugs are limited by the need of ultraviolet (UV) light, which is often damaging and not suitable for tissue penetration. Therefore, the development of photopharmacological agents triggered by visible light, especially near-infrared (NIR) light is highly desirable for future photoswitchable antibiotics. Herein, a novel photopharmacological antibacterial agent DTE-FQ was designed and synthesized by the incorporation of dithienylethene (DTE) molecular photoswitch and fluoroquinolones (FQ) antimicrobial drug norfloxacin bridged by pyridinium group and flexible butyl chain. As expected, as-prepared DTE-FQ presents efficient photoswitching behavior in various solutions upon alternating irradiation with blue light (460–470 nm) and NIR light (730–740 nm). Simultaneously, it shows significant and reversible configurational transition by the synergistic effect of DTE photoswitch and flexible butyl chain. Most remarkably, DTE-FQ reveals an at least 4-fold difference in activity against *Escherichia coli* (*E. coli*) for ring-open and ring-closed isomers, and a distinct change in bacterial growth is observed by *in situ* irradiation with NIR light in the presence of *E. coli*. These results are further confirmed by the molecular docking to DNA gyrase. The chain-like configuration of DTE-FQ treated with NIR light, inserted between the double-stranded DNA restraining the replication of DNA. Whereas the coiled configuration obtained by blue light irradiation, remained in the vicinity of the double-stranded DNA showing weak antibacterial activity. As far as we know, it represents the first example of blue-/NIR light-triggered photopharmacological antibacterial agent based on DTE switch so far, indicating its potential for *in vivo* photopharmacological applications.

© 2026 Published by Elsevier B.V. on behalf of Chinese Chemical Society and Institute of Materia Medica, Chinese Academy of Medical Sciences.

Conventional antibiotics used to treat bacterial infectious diseases are being compromised by the emergence of multidrug-resistant (MDR) bacteria, which stems from the excessive accumulation of antibiotics in the environment and organisms due to their overuse and misuse in healthcare and animal husbandry [1–5]. Besides, the common serious adverse effects are another plagues for long-term antibiotic therapy. For example, safety concerns regarding fluoroquinolones (FQ) as a class of synthetic and broad-spectrum antibiotics are still being raised as the Food and Drug Administration (FDA) announced in 2016 (*e.g.*, nerve damage, tendon rupture, and selection of resistant pathogens) [6,7]. Such a decline in the reliability of these traditional antibiotics is particularly troubling in the face of an increasing prevalence of MDR bacteria and a slower pace of antimicrobial innovation over the past five decades [8]. Therefore, exploring non-traditional therapeutic approaches to combat antibiotic resistance is urgently needed.

Fortunately, the emerging photopharmacology will provide a radical solution to systemic side effects and the drug resistance [9–23], in which the molecular photoswitch is commonly incorporated to externally control the biological activity of drug molecules *via* photoirradiation to facilitate high spatiotemporal precision treatment. In the current photopharmacological study, the azobenzene featured by *trans-cis* isomerization is the most frequently utilized

* Corresponding authors.
E-mail addresses: liziyong@mails.ccnu.edu.cn (Z. Li), yxg2233@126.com (X.-G. Yang), yinj@ccnu.edu.cn (J. Yin).
[1] These authors contributed equally to this work.

https://doi.org/10.1016/j.cclet.2025.111139
1001-8417/© 2026 Published by Elsevier B.V. on behalf of Chinese Chemical Society and Institute of Materia Medica, Chinese Academy of Medical Sciences.

photoswitches thanks to synthetic accessibility, robust photochemical performance and large change in geometry [24]. Scenarios of the successful utilization of photopharmacology based on azobenzene include vision restoration [25], antitumor therapy [26], ion channels [27], photoresponsive enzyme inhibitors [28], photocontrolled antimicrobials [29–31], and so forth. Although azobenzene-based photopharmacological agents have been extensively developed, the potential toxicity and thermodynamic instability have become limitations to their *in vivo* applications [32]. Additionally, poor cellular stability is also an ongoing concern since azobenzene is readily degraded to hydrazobenzene products by reduction of the intracellular glutathione (GSH, up to 10 mmol/L) [33]. As a consequence, the development of alternative photoswitches for azobenzene to prepare novel photopharmacological agents is highly desirable and remains a huge challenge.

As an alternative, dithienylethene (DTE), which can switch between ring-open and ring-closed isomers accompanying with changes in configuration and electronic structure, is appealing for photopharmacological applications due to their low toxicity, excellent thermal stability and robust fatigue resistance [34–39]. Against this backdrop, several photopharmacological agents bearing DTE photoswitch have been successfully developed in recent years, *e.g.*, anticancer therapy [40,41], photocontrolled enzyme inhibitor [42–46], insect receptor [47], and antimicrobials [48–50]. So far, however, relatively few investigation on DTE-based photopharmacology has been carried out despite their convincing photoswitching performance. In addition, the application of DTE switch in photopharmacology is mostly limited by the demand of ultraviolet (UV) light induced photoisomerization. UV light shows a limited tissue penetration depth and high toxicity to healthy cells [51,52]. More recent studies have been devoted to designing and exploiting visible light-driven DTE switches for potential biological applications [53–58]. The following general principles have been identified: upconverting nanoparticles, triplet sensitization, extended π-conjugation systems, multiphoton absorption, *etc*. Recently, our group has successfully developed a sequence of efficient visible/near-infrared (NIR) light-triggered DTE derivatives bearing electron-withdrawing difluoroboron β-diketonate (BF_2bdk) groups by "acceptor synergistic conjugation system" strategy (Fig. S1 in Supporting information) [56–58]. Inspired by these successful cases mentioned above, we speculate that incorporation of the conjugated DTE fragment with electron-withdrawing acceptor into certain drug molecule will be promising to obtain efficient visible/NIR light-excited photopharmacological agents based on DTE switch.

To validate this hypothesis, we have rationally designed and prepared a novel DTE-based photopharmacological antibacterial agent DTE-FQ (Fig. 1a) by incorporating conjugated DTE moiety with pyridinium acceptor into fluoroquinolone antimicrobial drug (norfloxacin), in which pyridinium group serves as both hydrophilic acceptor (A) and bacterial membrane-targeting moiety, and the butyl chain between DTE unit and norfloxacin acts as a flexible linker, respectively. In such photopharmacological system, the molecular design principle for the incorporation of pyridinium group has endowed DTE-FQ with four main superiorities: (I) Redshifting absorption wavelength by reducing orbital energy of the ring-open isomer, (II) extending excitation and emission wavelengths, (III) enhancing photoswitching performance and (IV) increasing water solubility and bacterial membrane-targeting ability. As expected, as-prepared DTE-FQ presents efficient photochromic properties and fluorescence switching behavior in solutions of different polarity upon alternating irradiation with blue light (460–470 nm) and NIR light (730–740 nm). Most remarkably, the ring-open isomer of DTE-FQ exhibits 4 times higher activity against *E. coli* (*E. coli*) compared to the ring-closed isomer after radiated by blue light. As far as we know, this represents the first case of blue-/NIR light-triggered photopharmacological antibacterial agent

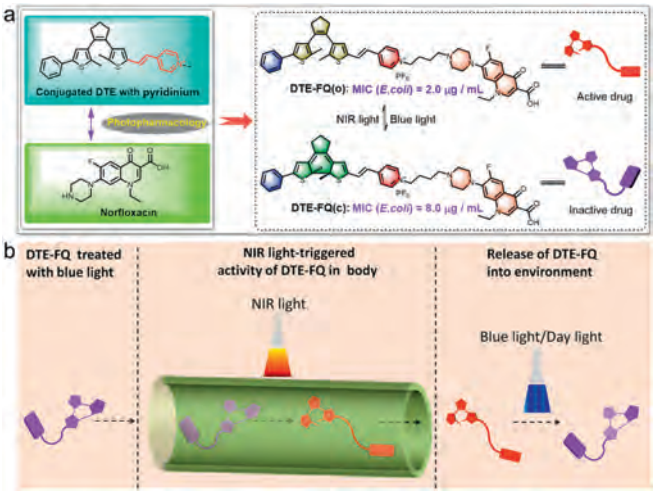


Fig. 1. (a) Design rationale of NIR light-triggered photopharmacological agent DTE-FQ by the incorporation of DTE molecular photoswitch and FQ derivative norfloxacin bridged by pyridinium group and flexible butyl chain. Radiated by blue and NIR light, it shows reversible transition of ring-closed DTE-FQ(c) and ring-open DTE-FQ(o) isomer respectively. (b) Schematic diagram of remote spatial and temporal control of bioactivity for DTE-FQ. When the inactive DTE-FQ(c) with coiled configuration reach to the site of action in body, radiation of NIR light can trigger the activity by the formation of DTE-FQ(o) with chain-like configuration. After release into environment, radiation of blue or day light can further induce the inactive DTE-FQ(c).

based on DTE switch, marking a significant advance in the reversible photocontrol of antibacterial agents *in vivo* with biocompatible NIR light in the therapeutic window. The as-prepared DTE-FQ also displays promising application prospect in the field of smart drugs. As illustrated in Fig. 1b, a low dose of DTE-FQ after treated by blue light are safe to healthy cells in the body. When this drug reached its site of action, it possesses antibacterial activity against *E. coli*. by *in situ* irradiated with NIR light. Therefore, the NIR light-triggered photoisomerization mode of DTE-FQ provides more safe and spatio-temporal controllable treatment in organisms.

According to the relationship between the structure and activity of FQ drugs [59], the N atom in the piperidine group of FQ is generally recognized as the modification site without loss of antibacterial potency. Hence, a novel DTE-based fluoroquinolone derivative (DTE-FQ) has been rationally designed by directly connecting pyridinium-functionalized conjugated DTE switch to norfloxacin *via* a flexible butyl chain. As depicted in Scheme S1 (Supporting information), the target DTE-FQ is prepared by the Knoevenagel condensation reaction between DTE-CHO (**3**) and 4-methyl pyridinium-subsituted norfloxacin (**5**) by using piperidine as a catalysis in anhydrous EtOH, followed by counter ion exchange with saturated aqueous NH_4PF_6 in a yield of 51 %. Its chemical structure is well characterized by ^{1}H nuclear magnetic resonance (NMR), ^{13}C NMR, high-resolution mass spectrometry (HRMS) and infrared (IR) spectrum (Figs. S24–S30 in Supporting information). From ^{1}H NMR spectrum of DTE-FQ, the coupling constants of the chemical shifts at 7.06 and 6.97 ppm assigned to carbon-carbon double bond are *ca.* 17.2 Hz, suggesting a stable trans-configuration for ethylene bond in DTE-FQ.

With this DTE-based fluoroquinolone derivative DTE-FQ in hand, its photoswitching behavior is subsequently explored in different polar solvents under alternating irradiation with blue light (460–470 nm) and NIR light (730–740 nm). As illustrated in Fig. 2a and Table 1, the ring-open isomer of DTE-FQ (denoted as DTE-FQ(o)) clearly shows a strong absorption peak at 448 nm ($\varepsilon = 2.86 \times 10^4$ L mol^{-1} cm^{-1}) in the visible region in

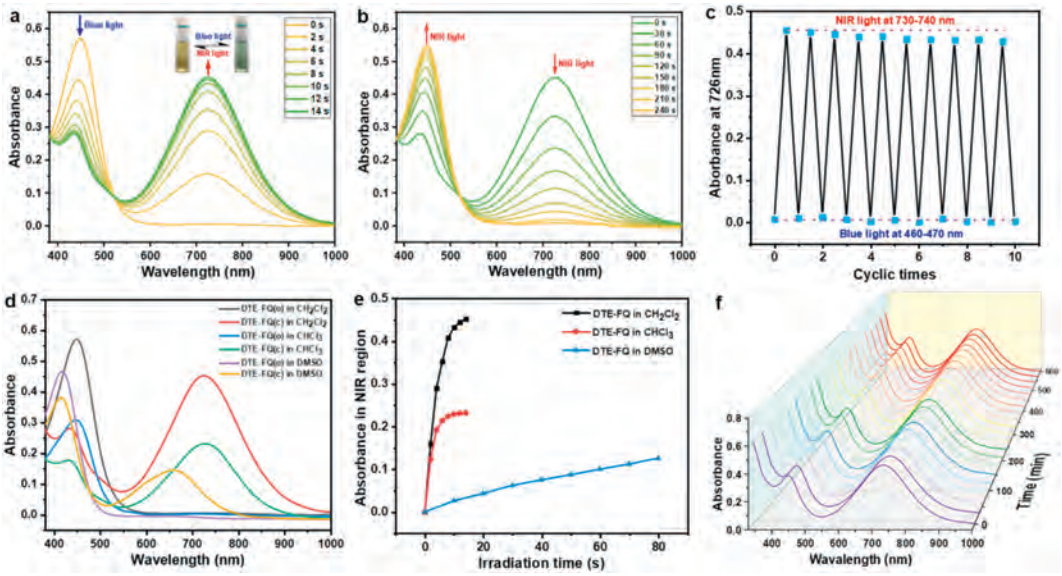


Fig. 2. The absorption spectra changes of DTE-FQ in dichloromethane (2.0×10^{-5} mol/L) upon alternating irradiation with blue light at 460–470 nm (a) and NIR light at 730–740 nm (b). The insets show the corresponding color changes upon photoirradiation. The fatigue resistance of DTE-FQ in dichloromethane for ten cycles (c). The absorption spectra of DTE-FQ before and after irradiation with blue light in various solvents (2.0×10^{-5} mol/L) (d). Optical response rate of DTE-FQ upon blue light irradiation in various solvents (2.0×10^{-5} mol/L) by monitoring changes in the maximum absorption wavelength (λ_{max}) of DTE-FQ(c) (e). The thermal stability of DTE-FQ in dichloromethane (2.0×10^{-5} mol/L) at 40 °C by monitoring changes in λ_{max} of DTE-FQ(c) at PSS (f).

Table 1
Photochromic and fluorescent parameters of DTE-FQ in various solvents (2.0×10^{-5} mol/L).

Solvents	$\lambda_{max}{}^{a}$ (nm) ($\varepsilon \times 10^{-4}$, L mol^{-1} cm^{-1})	$\lambda_{max}{}^{b}$ (nm) ($\varepsilon \times 10^{-4}$, L mol^{-1} cm^{-1})	$\varphi_{o\text{-}c}{}^{c}$	$\varphi_{c\text{-}o}{}^{d}$	$\lambda_{em}{}^{e}$ (nm)	$\Phi_f{}^{f}$	τ (ns)
CH_2Cl_2	448 (2.86)	726 (2.26)	0.37	0.008	590	0.18	0.77
$CHCl_3$	448 (1.55)	728 (1.17)	0.31	0.007	572	0.11	1.30
DMSO	418 (2.34)	662 (0.73)	0.075	0.008	540	0.07	0.40

[a] Absorption maxima of ring-open isomers.
[b] Absorption maxima of ring-closed isomers.
[c] Cyclization quantum yields.
[d] Cycloreversion quantum yields.
[e] Fluorescence emission maxima.
[f] Fluorescence quantum yield determined by a standard method with rhodamine 6G in water ($\Phi_{ref} = 0.75$, $\lambda_{ex} = 488$ nm) as the reference.

dichloromethane, which is derived from intramolecular charge transfer (ICT) transition between DTE moiety and pyridinium acceptor [60–63]. Upon irradiation with blue light, a NIR absorption band centered at 726 nm ($\varepsilon = 2.26 \times 10^4$ L mol^{-1} cm^{-1}) gradually appears accompanied with the color change from yellow to green (Fig. 2a, insets), indicating the conversion from ring-open isomer DTE-FQ(o) to ring-closed isomer DTE-FQ(c). Surprisingly, it takes 14 s for blue light irradiation to reach the photostationary state (PSS). Importantly, a clean isosbestic point at 522 nm pointing to high fatigue resistance is observed, suggesting a smooth transition of DTE-FQ(o) and DTE-FQ(c). Furthermore, NIR light excitation ($\lambda = 730$–740 nm, 180 s) of the green isomer triggers a cycloreversion reaction to regenerate its initial yellow isomer (Fig. 2b). Particularly, decent fatigue resistance can be observed by alternating irradiation of blue and NIR light ten times (Fig. 2c and Fig. S2 in Supporting information), probably due to the inhibition of photo-byproducts generation pathways under mild irradiation conditions. The cyclization and cycloreversion quantum yields of DTE-FQ in dichloromethane are recorded as $\varphi_{o\text{-}c} = 0.37$ and $\varphi_{c\text{-}o} = 0.008$, respectively (Table 1). When exposed to blue light and NIR/Red light, DTE-FQ presents similar photochromic behaviors in $CHCl_3$ and DMSO, as depicted in Figs. S3–S12 (Supporting information) and Table 1. In sharp contrast with that in DMSO, both open and closed isomers have a pronounced bathochromic shift in halogenated solvents with low polarity, *i.e.*, CH_2Cl_2 and $CHCl_3$ ($\Delta\lambda = 30$ nm for open form and $\Delta\lambda = 66$ nm for closed form, respectively) (Fig. 2d and Table 1). Such a large redshift can be attributed to the formation of *J*-aggregation in poor solvents with low polarity (CH_2Cl_2 and $CHCl_3$), as shown in Fig. S13 (Supporting information). Compared to those in $CHCl_2$ and DMSO, it undergoes a noticeable degradation after two cycles in $CHCl_3$, as shown in Fig. S6. In addition, it takes less time to reach PSS in low-polarity solvents (*i.e.*, 14 s in both CH_2Cl_2 and $CHCl_3$) compared to 100 s in DMSO, implying that the optical response rate of DTE-FQ in CH_2Cl_2 and $CHCl_3$ is much faster than that in DMSO (Fig. 2e). As expected, the corresponding $\varphi_{o\text{-}c}$ decreases as the polarity of the solvent increases (such as $\varphi_{o\text{-}c} = 0.37$ in CH_2Cl_2, $\varphi_{o\text{-}c} = 0.31$ in $CHCl_3$, and $\varphi_{o\text{-}c} = 0.075$ in DMSO). This is attributed to the fact that the excited state of the ring-open form in DMSO with large polarity dominates with the inactive twisted conformation with a large dipole moment [64,65]. Compared to the previously reported DTEs with the extended π-conjugation system [66,67], DTE-FQ with the acceptor synergistic conjugation system showcases a much bigger $\varphi_{o\text{-}c}$. In brief, DTE-FQ presents an exceptional blue/NIR light-triggered photochromic behavior in different solvents, in which the incorporation of norfloxacin fragment has little detectable effect on its photoswitching performance.

Subsequently, the photoisomerization of DTE-FQ is further evaluated *via* ^{1}H NMR spectral variations in DMSO–d_6. As depicted in Fig. S14 (Supporting information), the proton signals of thiophene groups in closed form DTE-FQ(c) ($\delta(H_a') = 6.66$ ppm, $\delta(H_e') = 6.89$ ppm) display an obvious upfield shift compared to

those of its corresponding open form DTE-FQ(o) ($\delta(H_a) = 7.25$ ppm, $\delta(H_e) = 7.32$ ppm), which is attributable to the electron shielding effect of closed form with an extended π-conjugation. According to ^{1}H NMR results, a photocyclization conversion ratio of 47.4% is determined at PSS. Moreover, thermal stability investigated in dark condition is an important criterion for evaluating the photoswitchable performance of photopharmacological agents [68]. As illustrated in Fig. 2f, the absorption spectra of DTE-FQ at PSS remains almost the same after keeping in dark for 600 min at 40 °C, revealing its good thermal stability and a larger ground state activation energy difference that is not conducive to thermal state activation energy difference that is not conducive to thermal cycloreversion reaction. Moreover, the thermal half-life time is estimated to be 142 h in CH_2Cl_2, 185 h in $CHCl_3$ and 172 h in DMSO at 40 °C (Fig. S15 in Supporting information).

Considering intense emission performance of norfloxacin, the subsequent investigations are focused on fluorescent switching behavior in three various solvents. As depicted in Figs. 3a and b, a bright orange-yellow fluorescence with the maximum emission at 590 nm for the open isomer DTE-FQ(o) is observed prior to irradiation and relative fluorescence quantum yield is estimated to be $\Phi_f = 0.18$ in dichloromethane. When irradiated with blue light at 460–470 nm, the emission intensity at 590 nm is gradually decreased along with the fading of orange-yellow fluorescence and a detectable blue shift of the maximum emission wavelength (Fig. 3g), which can be attributed to the re-absorption process of the fluorescence. At PSS, the emission intensity of DTE-FQ(o) is only quenched by *ca.* 56% due to partial overlap between the emission spectrum of DTE-FQ(o) and absorption spectrum of DTE-FQ(c) (Fig. 3d). The irradiation of NIR light (730–740 nm) triggers the original orange-yellow emission resulting from the formation of DTE-FQ(c) (Fig. 3c). As shown in Figs. S16 and S17 (Supporting information), similar fluorescent switching process is detected in $CHCl_3$ and DMSO under the same light irradiation. Compared to that in CH_2Cl_2, the emission peak of DTE-FQ(o) displays a significant hypochromatic shift in $CHCl_3$ and DMSO ($\Delta\lambda = 18$ and 50 nm, respectively) (Fig. 3e and Table 1), which is basically consistent with the change of absorption spectra. Meanwhile, the time-resolved decay curves reveals that DTE-FQ(o) has shorter lifetime ranging from $\tau = 0.40$–1.30 ns in three different solvents (Fig. 3f and Table 1). In brief, DTE-FQ exhibits solvent-dependent fluorescent switching behaviors.

To further gain deeper insight into blue light-driven photoswitching behaviors of DTE-FQ, density functional theory (DFT) calculations are performed to explore electronic properties and the optimized geometries of its open and closed isomers at the B3LYP/6–31G* level using the Gaussian 09 program [69]. As depicted in Fig. 4a, the highest occupied molecular orbital (HOMO) orbital energy of DTE-FQ(o) is mainly localized around the left thiophene and benzene groups, whereas its lowest unoccupied molecular orbital (LUMO) is largely distributed over the right thiophene and electron-deficient pyridinium moieties linked by the vinyl bond. Such partially separated HOMO and LUMO orbitals indicates that ICT transition can occur between the pyridinium acceptor and DTE donor in the excited state, which endows with the ability to excite photocyclization by visible light. For DTE-FQ(c), the HOMO is distributed on the central DTE core and groups directly connected on its both sides. As expected, a narrower energy band gap ($E_g = 1.75$ eV) for DTE-FQ(c) is detected in comparison to DTE-FQ(o) ($E_g = 2.64$ eV) as a result of the extended π conjugation system for closed form. Based on their optimized molecular structures, the calculated electrostatic potential (ESP) analysis of both DTE-FQ(o) and DTE-FQ(c) is conducted to verify the potential binding process and change in the dipole moment. ESP surfaces from Fig. 4b indicate that the positive π-charge is mainly distributed in the pyridinium group, which will tend to bind with the negative bacterial membrane *via* electrostatic interactions. Noticeably, an enhanced dipole moment for DTE-FQ(c) is determined

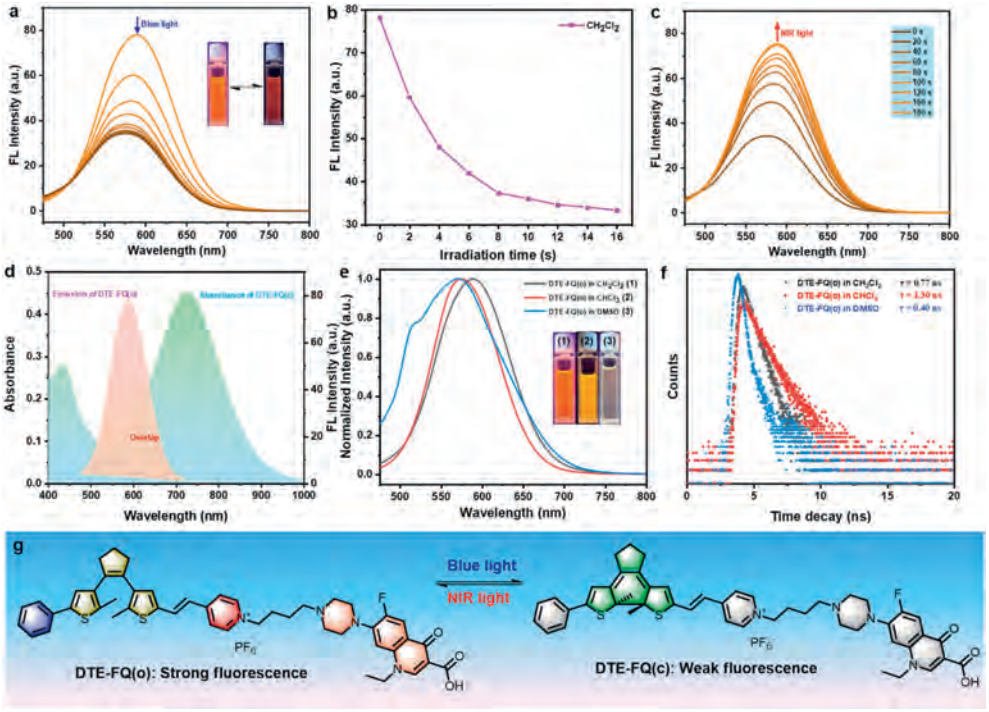


Fig. 3. The fluorescence spectra changes of DTE-FQ in dichloromethane (2.0×10^{-5} mol/L) upon alternating irradiation with blue light at 460–470 nm (a, b) and NIR light at 730–740 nm (c) ($\lambda_{ex} = 450$ nm, slit width (Ex and Em): 10.0 nm). (Inset) Corresponding fluorescent color changes upon photoirradiation. The emission spectrum of DTE-FQ(o) and absorption spectrrum of DTE-FQ(c) (d). The normalized fluorescence spectra of DTE-FQ(o) in various solvents (2.0×10^{-5} mol/L) before photoirradiation (e) (slit width (Ex and Em): 10.0 nm). (Inset) Corresponding fluorescence photographs before photoirradiation. The fluorescence decay curves of DTE-FQ(o) in various solvents (f). Photochromic reaction of DTE-FQ along with changes in fluorescence (g).

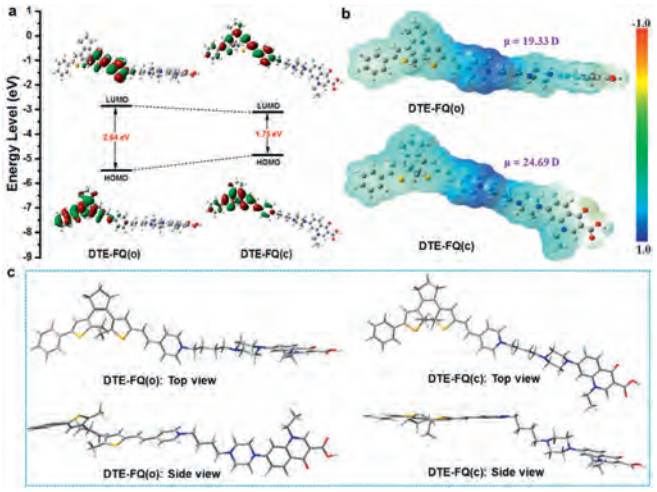


Fig. 4. Frontier molecular orbital profiles of DTE-FQ(o) and DTE-FQ(c) (a), the calculated electrostatic potential surfaces of DTE-FQ(o) and DTE-FQ(c) (blue region represents the positive work and the red region represents the negative work) (b), and the energy-minimized structures of DTE-FQ(o) and DTE-FQ(c) (c) based on DFT calculations at the B3LYP/6–31G* level using the Gaussian 09 program.

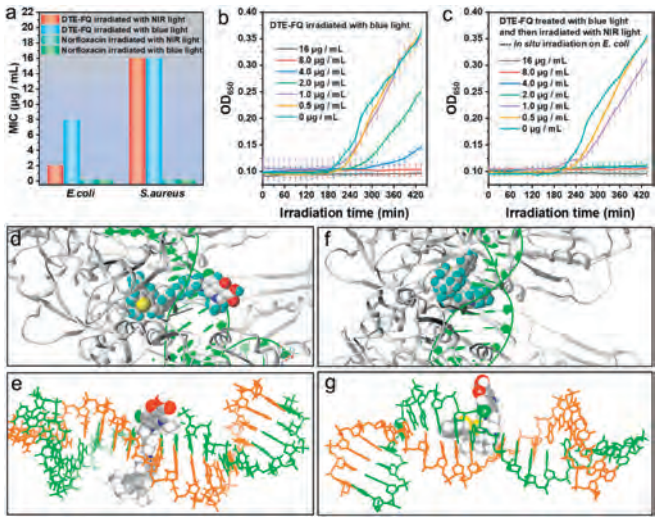


Fig. 5. (a) The antibacterial activity (MIC) of DTE-FQ and norfloxacin (treated with blue or NIR light) against *E. coli* ATCC 25,922 and *S. aureus* ATCC6538. Bacterial growth curves of *E. coli* ATCC 25,922 at increasing concentrations of DTE-FQ, samples after irradiation with blue light (b) and samples treated with blue light and then *in situ* irradiation with NIR light (λ = 730–740 nm) in the presence of bacteria (c). Error bars show standard deviation calculated from measurements in triplicate. The docking of the open isomer DTE-FQ(o) (d, e) and closed isomer DTE-FQ(c) (f, g) to DNA gyrase. The PDB protein data of DNA is used for the molecular docking study (PDB code: 2XCS, https://www.pdbus.org/structure/2XCS). And the protein is optimized for hydrogenation and protonation before docking.

to be 24.69 D compared to that of DTE-FQ(o) (μ = 19.33 D), implying an obvious polarity change during photoisomerization. As illustrated in Fig. 4c, the energy-minimized structure of DTE-FQ(o) displays a classical antiparallel conformation, which is conducive to the photocyclization reaction. From side view of DTE-FQ(o), the plane of DTE unit is almost perpendicular to the plane of norfloxacin, and two planes tend to be approximately parallel after cyclization. Thereby it indicates a large change in configuration due to the presence of flexible C4 chains before and after irradiation, which will be of great significance for the photocontrol of antimicrobial activity. Consequently, the DFT calculations further validate the above photochromic experiment results and has certain guiding significance for the evaluation of the difference in antibacterial activity.

The excellent blue/NIR light-excited photoswitchable behavior and apparent changes in polarity and configuration during photoisomerization inspire us to further investigate antimicrobial activity *in vitro* of DTE-FQ before and after irradiation with blue light. Accordingly, Gram-positive *Staphylococcus aureus* (*S. aureus*) and Gram-negative *E. coli* (*E. coli*) are employed to evaluate its reversible antimicrobial performance by the standard broth dilution method. As depicted in Fig. 5a, DTE-FQ after NIR light irradiation (minimum inhibitory concentration (MIC) = 2.0 μg/mL) shows 4 times higher activity against *E. coli* than that irradiated with blue light (MIC = 8.0 μg/mL). Whereas, almost the same lower antimicrobial activity against *S. aureus* (MIC = 16 μg/mL) was detected under the same conditions abovementioned. In comparison, norfloxacin displays more antibacterial activity (MIC = 0.125 μg/mL) against both *S. aureus* and *E. coli*. Notwithstanding, there are no differences after blue/NIR light irradiation for norfloxacin. From the perspective of practical applications, the NIR light-controlled antimicrobial activity of DTE-FQ molecular switch shows higher spatiotemporal precision treatment and more safety to organism. To verify this point, antibacterial experiments of DTE-FQ after blue light irradiation were performed in the presence of *E. coli*. The bacterial growth curves exhibit that low dose (2.0 μg/mL for example) of DTE-FQ has no antimicrobial activity against *E. coli* (Fig. 5b). When *in situ* irradiation with NIR light, it shows efficient inhibition of bacterial growth (Fig. 5c). Therefore, these experimental results indicates that ring-open isomerization of DTE-FQ can be achieved by nontoxic NIR light with affecting bacterial growth. This marks a significant advance in the reversible photocontrol of antibacterial agents *in vivo* with biocompatible NIR light located in the therapeutic window. As far as we know, it represents the first example of blue-/NIR light-triggered photopharmacological antibacterial agent based on DTE switch so far, indicating its potential for *in vivo* photopharmacological applications. Besides, the 460–470 nm blue light employed to drive open-to-closed isomerization coincides with the highest intensity region of natural day light. Accordingly, day light can also be utilized to trigger the photocyclization reaction (Fig. S18 in Supporting information). It is hereby predicted that radiation of day light can induce the inactive DTE-FQ(c) after release into environment.

Whereafter, the molecular docking of DTE-FQ to DNA gyrase (one of type IIA topoisomerases) is carried out at the Sybyl X software V2.0 in order to rationally expound the discrepancy in antibacterial activity of both open and closed forms. Before molecular docking, all the proteins in PDB protein data of DNA are optimized for hydrogenation and protonation [70,71]. From Figs. 5d and e and Fig. S19 (Supporting information), the norfloxacin fragment of the open isomer DTE-FQ(o) is capable of insert between the double-stranded DNA probably due to its suitable configuration (Fig. S20 in Supporting information) and some weak interactions with the DNA base, which favors cleaving DNA and thus inhibiting the replication of DNA. In comparison, the coiled configuration of DTE-FQ(c) in the docking system leaves the antimicrobial molecule remaining only in the vicinity of the double-stranded DNA (Figs. 5f and g, Figs. S21 and S22 in Supporting information), so this will be detrimental to exert the effect of DTE-FQ(c) on DNA replication. Besides, we identify 15 active-site residues in the PDB protein that interact with DTE-FQ(o) and DTE-FQ(c) at high frequencies (Fig. S23 in Supporting information), respectively, although the difference is less pronounced. In brief, the docking results provides a rationale for significant difference in antibacterial activity between the two photoisomeric states DTE-FQ. This is an obvious prerequisite for the light-triggered photopharmacology.

In summary, we have successfully developed a novel DTE-based photopharmacological antibacterial agent (DTE-FQ) by incorpora-

tion of the conjugated DTE moiety with pyridinium acceptor into norfloxacin. The combination of experiments and theoretical calculations reveal the following results: Firstly, the synergistic effect of the DTE photoswitch and flexible butyl chain can lead to significant change in molecular configuration for DTE-FQ. The ring-open state of DTE-FQ with proximate chain-like configuration can insert between the double-stranded DNA restraining the replication of DNA, whereas the ring-closed isomer exhibiting coiled configuration and large steric hindrance remained in the vicinity of the double-stranded DNA. Secondly, the positively charged pyridinium group tends to bind with the negative bacterial membrane *via* electrostatic interactions. More importantly, the electron-deficient pyridinium moiety linked with vinyl bond not only promotes the photocyclization efficiency, but also extends the triggered cycloreversion reaction to NIR light region. Photopharmacological experiments show that the DTE-FQ antibacterial agent treated by blue light has no antibacterial activity against *E. coli* in a low dose (2.0 μg/mL). *In situ* irradiated with NIR light, the bacterial growth can be efficiently inhibited. Therefore, this work not only provides an effective way to trigger the antibacterial activity of photopharmacological agents by NIR light, solving the problem of tissue penetration and high toxicity to healthy cells from UV light, but also displays promising application prospect of safe and spatiotemporal precision treatment through remote light control. As we have seen, this represents the first case of blue-/NIR light-triggered photopharmacological antibacterial agent based on DTE switch so far, marking a significant advance in the reversible photocontrol of antibacterial agents *in vivo* with biocompatible NIR light in the therapeutic window.

Declaration of competing interest

The authors declare that they have no known competing financial interests or personal relationships that could have appeared to influence the work reported in this paper.

CRediT authorship contribution statement

Ziyong Li: Writing – original draft, Investigation, Conceptualization. **Jinzhao Song:** Methodology, Investigation, Data curation. **Qilian Wang:** Investigation, Data curation. **Yueheng Qi:** Software, Methodology. **Xingrui Gao:** Methodology, Formal analysis. **Yongliang Feng:** Project administration, Investigation. **Haining Zhang:** Resources, Project administration. **Ying-Jun Chen:** Software, Formal analysis. **Hui Guo:** Validation, Funding acquisition. **Xiao-Gang Yang:** Writing – review & editing, Funding acquisition. **Jun Yin:** Writing – review & editing, Supervision.

Acknowledgments

This work was supported by the National Natural Science Foundation of China (No. 22371109), Science Fund for Distinguished Young Scholars in Henan Province (No. 242300421036), Science and Technology Key Research Project of Henan Province (Nos. 252102311211 and 242102230119), and Innovation and Entrepreneurship Training Program for College students in China (Nos. 202310482001 and 202410482001).

Supplementary materials

Supplementary material associated with this article can be found, in the online version, at doi:10.1016/j.cclet.2025.111139.

References

[1] E. Svoboda, Nature 586 (2020) S58.
[2] X. Li, H. Bai, Y. Yang, et al., Adv. Mater. 31 (2019) 1805092.
[3] J. Carlet, P. Collignon, D. Goldmann, et al., Lancet 378 (2011) 369–371.
[4] J.A. Bartell, L.M. Sommer, J.A. Haagensen, et al., Nat. Commun. 10 (2019) 629.
[5] Z. Li, J. Song, X. Gao, et al., Chin. Chem. Lett. 36 (2025) 110073.
[6] A.J. Mehlhorn, D.A. Brown, Ann. Pharmacother. 41 (2007) 1859–1866.
[7] U. S. Food and Drug Administration, FDA updates warnings for fluoroquinolone antibiotics. https://www.fda.gov/NewsEvents/Newsroom/PressAnnouncements/ucm513183.htm, July 26, 2016 (accessed March 3, 2017).
[8] K. Lewis, Nat. Rev. Drug Discov. 12 (2013) 371–387.
[9] M.J. Fuchter, J. Med. Chem. 63 (2020) 11436–11447.
[10] K. Hull, J. Morstein, D. Trauner, Chem. Rev. 118 (2018) 10710–10747.
[11] W.A. Velema, W. Szymanski, B.L. Feringa, J. Am. Chem. Soc. 136 (2014) 2178–2191.
[12] M.M. Lerch, M.J. Hansen, G.M. van Dam, W. Szymanski, B.L. Feringa, Angew. Chem. Int. Ed. 55 (2016) 10978–10999.
[13] J. Broichhagen, J.A. Frank, D. Trauner, Acc. Chem. Res. 48 (2015) 1947–1960.
[14] W. Szymanski, J.M. Beierle, H.A. Kistemaker, W.A. Velema, B.L. Feringa, Chem. Rev. 113 (2013) 6114–6178.
[15] K. An, Q. Qiao, Lovelesh, et al., Chin. Chem. Lett. 36 (2025) 109786.
[16] Y. Xiang, W. Xiong, Z. Yang, et al., Chem. Eng. J. 486 (2024) 149979.
[17] I.M. Welleman, M.W. Hoorens, B.L. Feringa, H.H. Boersma, W. Szymański, Chem. Sci. 11 (2020) 11672–11691.
[18] Z. Zhang, G.N.T. Le, Y. Ge, et al., Nat. Chem. 15 (2023) 1285–1295.
[19] A.C. Kneuttinger, Biol. Chem. 403 (2022) 573–613.
[20] B. Zhu, X. Yang, L. Jiang, et al., Chin. Chem. Lett. 36 (2025) 110222.
[21] A. Mukherjee, M.D. Seyfried, B.J. Ravoo, Angew. Chem. Int. Ed. 62 (2023) e202304437.
[22] M.W. Hoorens, W. Szymanski, Trends Biochem. Sci. 43 (2018) 567–575.
[23] E. Bamberg, W. Gärtner, D. Trauner, Chem. Rev. 118 (2018) 10627–10628.
[24] Y. Huang, X. Zeng, X. Ma, et al., Nat. Commun. 15 (2024) 8670.
[25] L. Laprell, K. Hull, P. Stawski, et al., ACS Chem. Neurosci. 7 (2016) 15–20.
[26] M. Borowiak, W. Nahaboo, M. Reynders, et al., Cell 162 (2015) 403–411.
[27] A. Nin-Hill, N.P.F. Mueller, C. Molteni, C. Rovira, M. Alfonso-Prieto, Int. J. Mol. Sci. 22 (2021) 12072.
[28] D. Laczi, M.D. Johnstone, C.L. Fleming, Chem. Asian J. 17 (2022) e202200200.
[29] W.A. Velema, J.P. Van Der Berg, M.J. Hansen, et al., Nat. Chem. 5 (2013) 924–928.
[30] M. Wegener, M.J. Hansen, A.J. Driessen, W. Szymanski, B.L. Feringa, J. Am. Chem. Soc. 139 (2017) 17979–17986.
[31] M.J. Hansen, J.I. Hille, W. Szymanski, A.J. Driessen, B.L. Feringa, Chem 5 (2019) 1293–1301.
[32] M.A. Brown, S.C. De Vito, Crit. Rev. Environ. Sci. Technol. 23 (1993) 249–324.
[33] C. Boulègue, M. Löweneck, C. Renner, L. Moroder, ChemBioChem 8 (2007) 591–594.
[34] O. Babii, S. Afonin, A.Y. Ishchenko, et al., J. Med. Chem. 61 (2018) 10793–10813.
[35] J. Zhang, J. Wang, H. Tian, Mater. Horiz. 1 (2014) 169–184.
[36] H. Cheng, J. Yoon, H. Tian, Coord. Chem. Rev. 372 (2018) 66–84.
[37] A.S. Lubbe, W. Szymanski, B.L. Feringa, Chem. Soc. Rev. 46 (2017) 1052–1079.
[38] Z. Li, S. Chen, Y. Huang, et al., Chem. Eng. J. 450 (2022) 138087.
[39] Z. Li, X. Zeng, C. Gao, et al., Coord. Chem. Rev. 497 (2023) 215451.
[40] A. Presa, R.F. Brissos, A.B. Caballero, et al., Angew. Chem. Int. Ed. 54 (2015) 4561–4565.
[41] O. Babii, S. Afonin, L.V. Garmanchuk, et al., Angew. Chem. Int. Ed. 55 (2016) 5493–5496.
[42] D. Vomasta, C. Högner, N.R. Branda, B. König, Angew. Chem. Int. Ed. 47 (2008) 7644–7647.
[43] D. Vomasta, A. Innocenti, B. König, C.T. Supuran, Bioorg. Med. Chem. Lett. 19 (2009) 1283–1286.
[44] X. Chen, S. Wehle, N. Kuzmanovic, et al., ACS Chem. Neurosci. 5 (2014) 377–389.
[45] C. Falenczyk, M. Schiedel, B. Karaman, et al., Chem. Sci. 5 (2014) 4794–4799.
[46] D. Lachmann, C. Studte, B. Männel, et al., Chem. Eur. J. 23 (2017) 13423–13434.
[47] W. Fu, Z. Li, X. Shao, Adv. Agrochem. 2 (2023) 142–153.
[48] O. Babii, S. Afonin, M. Berditsch, et al., Angew. Chem. Int. Ed. 53 (2014) 3392–3395.
[49] L. Tang, J. Li, Z. Yu, J. Meng, J. Li, Chem. Eng. J. 493 (2024) 152688.
[50] H. Zhang, Y. Qi, X. Zhao, et al., J. Org. Chem. 87 (2022) 7446–7455.
[51] R. Weissleder, Nat. Biotechnol. 19 (2001) 316–317.
[52] Y. Matsumura, H.N. Ananthaswamy, Toxicol. Appl. Pharmacol. 195 (2004) 298–308.
[53] C.C. Ko, V.W.W. Yam, Acc. Chem. Res. 51 (2018) 149–159.
[54] H. Wang, H.K. Bisoyi, X. Zhang, F. Hassan, Q. Li, Chem. Eur. J. 28 (2022) e202103906.
[55] Z. Zhang, W. Wang, M. O'Hagan, et al., Angew. Chem. Int. Ed. 61 (2022) e202205758.
[56] Z. Li, Y. Xie, M. Zhu, et al., Opt. Mater. 94 (2019) 257–265.
[57] Z. Li, J.R. Zhang, X.K. Tian, et al., Chem. Sci. 13 (2022) 9381–9386.
[58] Z. Li, X. Ma, J. Song, et al., Chem. Sci. 16 (2025) 1762–1771.
[59] D.C. Hooper, E. Rubinstein, Quinolone Antimicrobial Agents, 3rd ed., ASM Press, Washington, D.C., 2003.
[60] Z. Li, Q. Qiao, N. Xu, et al., Chin. Chem. Lett. 35 (2024) 108824.
[61] Z. Li, J. Song, Q. Wang, et al., Mater. Chem. Front. 9 (2025) 234–242.
[62] T. Shi, X. Chen, X. Zhou, et al., Chin. Chem. Lett. 36 (2025) 110408.
[63] Z. Li, Y. Song, Y. Dai, et al., Opt. Mater. 95 (2019) 109235.
[64] M. Irie, K. Sayo, J. Phys. Chem. 96 (1992) 7671–7674.

[65] Y. Ishibashi, T. Umesato, M. Fujiwara, et al., J. Phys. Chem. C 120 (2016) 1170–1177.
[66] T. Fukaminato, T. Hirose, T. Doi, et al., J. Am. Chem. Soc. 136 (2014) 17145–17154.
[67] F. Hu, M. Cao, X. Ma, S.H. Liu, J. Yin, J. Org. Chem. 80 (2015) 7830–7835.
[68] X. Hu, J. Zhao, Z. Wang, et al., Dyes Pigm. 205 (2022) 110571.
[69] M.J. Frisch, G.W. Trucks, H.B. Schlegel, et al., Gaussian 09, Revision B.01, Gaussian Inc, Wallingford CT, 2010.
[70] I. Laponogov, M.K. Sohi, D.A. Veselkov, et al., Nat. Struct. Mol. Biol. 16 (2009) 667–669.
[71] B.D. Bax, P.F. Chan, D.S. Eggleston, et al., Nature 466 (2010) 935–940.